

# Rethinking Sensors Modeling: Hierarchical Information Enhanced Traffic Forecasting

Qian Ma\*  
City University of Hong Kong  
qma233-c@my.cityu.edu.hk

Zijian Zhang\*  
Jilin University  
City University of Hong Kong  
zhangzj2114@mails.jlu.edu.cn

Xiangyu Zhao†  
City University of Hong Kong  
xianzhao@cityu.edu.hk

Haoliang Li  
City University of Hong Kong  
haoliali@cityu.edu.hk

Hongwei Zhao†  
Jilin University  
zhaohw@jlu.edu.cn

Yiqi Wang  
Michigan State University  
wangy206@msu.edu

Zitao Liu  
Guangdong Institute of Smart  
Education, Jinan University  
liuzitao@jnu.edu.cn

Wanyu Wang  
City University of Hong Kong  
wanyuwang4-c@my.cityu.edu.hk

## ABSTRACT

With the acceleration of urbanization, traffic forecasting has become an essential role in smart city construction. In the context of spatio-temporal prediction, the key lies in how to model the dependencies of sensors. However, existing works basically only consider the micro relationships between sensors, where the sensors are treated equally, and their macroscopic dependencies are neglected. In this paper, we argue to rethink the sensor's dependency modeling from two hierarchies: regional and global perspectives. Particularly, we merge original sensors with high intra-region correlation as a region node to preserve the inter-region dependency. Then, we generate representative and common spatio-temporal patterns as global nodes to reflect a global dependency between sensors and provide auxiliary information for spatio-temporal dependency learning. In pursuit of the generality and reality of node representations, we incorporate a Meta GCN to calibrate the regional and global nodes in the physical data space. Furthermore, we devise the cross-hierarchy graph convolution to propagate information from different hierarchies. In a nutshell, we propose a Hierarchical Information Enhanced Spatio-Temporal prediction method, Hiest, to create and utilize the regional dependency and common spatio-temporal patterns. Extensive experiments have verified the leading performance of our Hiest against state-of-the-art baselines. We publicize the code to ease reproducibility<sup>1</sup>.

\*Both authors contributed equally to this research.

†Xiangyu Zhao and Hongwei Zhao are the corresponding authors.

<sup>1</sup><https://github.com/VAN-QIAN/CIKM23-Hiest>

Permission to make digital or hard copies of all or part of this work for personal or classroom use is granted without fee provided that copies are not made or distributed for profit or commercial advantage and that copies bear this notice and the full citation on the first page. Copyrights for components of this work owned by others than the author(s) must be honored. Abstracting with credit is permitted. To copy otherwise, or republish, to post on servers or to redistribute to lists, requires prior specific permission and/or a fee. Request permissions from [permissions@acm.org](mailto:permissions@acm.org).  
*CIKM '23, October 21–25, 2023, Birmingham, United Kingdom*  
© 2023 Copyright held by the owner/author(s). Publication rights licensed to ACM.  
ACM ISBN 979-8-4007-0124-5/23/10...\$15.00  
<https://doi.org/10.1145/3583780.3614910>

## CCS CONCEPTS

• Information systems → Traffic analysis; Spatial-temporal systems; • Computing methodologies → Neural networks.

## KEYWORDS

smart city, spatio-temporal prediction, graph learning

### ACM Reference Format:

Qian Ma, Zijian Zhang, Xiangyu Zhao, Haoliang Li, Hongwei Zhao, Yiqi Wang, Zitao Liu, and Wanyu Wang. 2023. Rethinking Sensors Modeling: Hierarchical Information Enhanced Traffic Forecasting. In *Proceedings of the 32nd ACM International Conference on Information and Knowledge Management (CIKM '23)*, October 21–25, 2023, Birmingham, United Kingdom. ACM, New York, NY, USA, 10 pages. <https://doi.org/10.1145/3583780.3614910>

## 1 INTRODUCTION

Intelligent Transportation Systems (ITS) play a critical role in smart city construction. Thanks to the promising progress of intelligent sensors, the collected extensive traffic data has unprecedentedly supported urban data mining research, such as traffic flow prediction [1, 6, 46], arriving time estimation [12, 26, 39], traffic speed analysis [2, 3, 5, 11] *etc.* Spatio-temporal prediction aims to analyze historical spatio-temporal properties and predict future trends [41, 41–43]. Inspired by the advancing capacity of representation learning of deep models, existing methods incorporate Temporal Convolution Networks (TCN) [10, 31], Recurrent Neural Networks (RNN) [16, 40], and self-attention mechanism [8, 45] for temporal variation capture. Convolutional Neural Networks (CNN) [9, 15, 37, 38] and Graph Neural Networks (GNN) [13, 16, 19, 20, 31] are generally utilized for spatial relationship learning.

To predict the traffic states of numerous sensors in a city, the key to solving spatio-temporal prediction is to capture the complex dependency among the sensors. However, although having shown promising effectiveness, current solutions [16, 23, 30, 42, 44, 45] of spatio-temporal prediction treat each sensor equally in sensor dependency modeling and essentially neglect the dependencies among nonadjacent sensors [7, 32]. Sensors from different regions own similar or distinct properties, and considering sensors equally

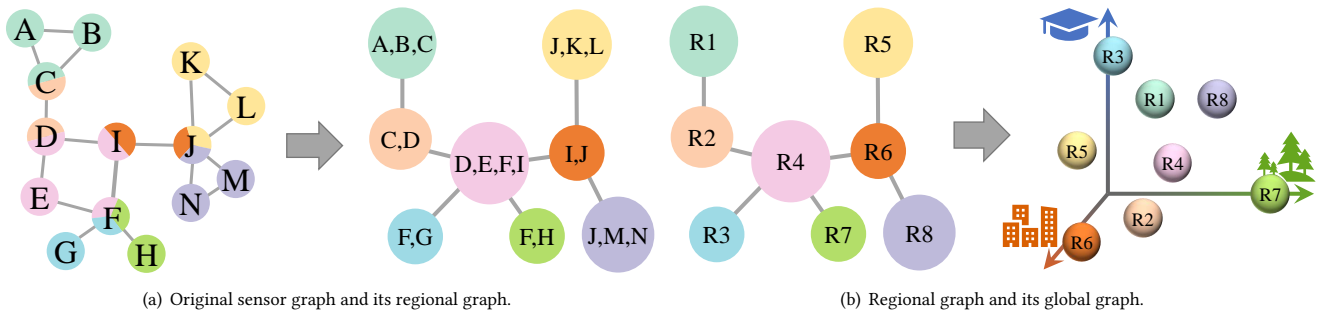


**Figure 1: Illustration of the original sensor graph and two hierarchical perspectives. (a) Sensors with the same color belong to the same bi-connected component and can be merged from the regional perspective. Cut-vertices containing multiple colors are assigned to all corresponding regions. (b) Considering the properties of regions (such as functions), regions can be described by global nodes with common and representative spatio-temporal patterns as base vectors.**

undermines the macro dependency learning. In this paper, we argue to rethink the dependency modeling of different sensors. We propose two hierarchical perspectives to depict the hierarchical dependencies among sensors, *i.e.*, regional and global perspectives.

**Regional perspective.** Sensors always share high-correlated properties with neighbors but weak relationships with others [7]. For example, sensors from the same county generally report similar traffic attributes since vehicles in the community flow in a relatively settled manner. Conversely, sensors maintain weak ties with the ones in other counties due to their unstable relationship. Modeling the regional dependency properly can provide a hierarchical perspective to describe the sensor relationship and benefits the information propagation among sensors.

**Global perspective.** Sensors own common spatio-temporal properties considering the function of their region [29, 33]. Traffic attributes recorded near schools should be different from those near natural parks because the weekday traffic in the educational areas varies regularly, but in recreation areas, the weekend traffic remarkably tops the weekdays. Moreover, different sensors from different educational areas are prone to have similar traffic attributes, *e.g.*, similar peaks and valleys of traffic flow variation in a day due to their similar traffic variation patterns. Hence, producing common and representative spatio-temporal patterns of sensors can offer auxiliary information to spatio-temporal modeling.

Basically, GCN-based methods [16, 30, 31, 34, 40, 45] are representative solutions to model sensor relationships. DCRNN [16] introduces diffusion convolution to propagate information in the graph. To dynamically describe the dependencies of sensors, GWNet [31] generates adaptive adjacency matrices. Nevertheless, this series of works treats all fine-grained sensors equally regardless of the macro dependency among the sensors and their high-order neighbors. Recently, efforts have been exerted to explore hierarchical sensor modeling [7, 17, 18, 28, 29, 32]. HGCN [7] devises a hierarchical view based on the fine-grained sensors by simply clustering the node representations. To maintain the information from high-order neighbors, Traffic-Transformer [32] resorts to masking the attention mechanism with high-order adjacency matrices. ST-HSL [17] introduces a hyper-graph to address the macro relationship of sensors. However, these methods build hierarchical views based

on the node representations and demand tremendous computational overhead for clustering. Besides, they neglect the important topological relationship, suffer from poor interpretability, and the performance depends on the manually designed architecture.

To achieve the goals above, we identify several key research questions to be tackled. (i) *How to formulate the macro dependency of sensors?* (ii) *How to attain the common and representative spatio-temporal patterns across the city?* (iii) *How to enhance spatio-temporal prediction given the macro dependency and representative spatio-temporal patterns of sensors?* Conquering these challenges is far from trivial. Given the numerous sensors with diverse properties: (i) Clustering the node representations lacks an understanding of graph structure, and the performance depends on the manually tuned architecture; (ii) Manual selection of representative sensors is impractical, and the generality and reality of spatio-temporal patterns are difficult to guarantee; (iii) Most importantly, there is still a lack of a solution orchestrating the hierarchical information with the original sensor graph and consolidating the spatio-temporal dependency modeling effectively.

In this paper, we present a **Hierarchical Information Enhanced Spatio-Temporal prediction method, HIEST**, to solve the research questions from the following three aspects. *Firstly, we propose to merge sensors with high local connectivity and achieve the graph of a regional perspective.* Specifically, instead of clustering nodes regardless of graph structure as in existing methods, we solve the Bi-Connected Component (BCC) of a graph, as in Figure 1 (a), and combine sensors belonging to the same BCC as the regional graph. We also assign the cut-vertex to the corresponding groups respectively, *e.g.*, node J is merged into all the related three groups, which further preserves the information propagation between sensors. *Based on the regional graph, we further extract general spatio-temporal patterns across the city with an orthogonal constraint to keep the distinctions.* Through a meta graph convolution network, we generate representative sensors in the physical data space to maintain reality and generality. These global nodes can serve as base vectors representing regions with diverse properties, as shown in Figure 1 (b). Furthermore, *we devise a Cross-Hierarchy Graph Convolutional Network, CHGCN, to enhance spatio-temporal prediction utilizing the merged sensors and general patterns.* Our Meta GCN embeds

the nodes in the original graph, regional graph, and global graph into the same feature space, to describe the spatio-temporal representation of the two hierarchical perspectives in the physical data space. Compared to existing hierarchical spatio-temporal prediction methods, the two hierarchies in Hiest owns physical meaning and good interpretability. We construct regional nodes according to the topological structure, and maintain the hierarchical nodes in the physical data space. Our main contributions are as follows:

- We reformulate spatio-temporal prediction with two hierarchical perspectives, *i.e.*, regional and global graphs, to capture the macro dependencies and common spatio-temporal patterns among sensors, respectively, which enjoy good interpretability.
- We devise a cross-hierarchy graph representation learning schema to incorporate hierarchical graphs in sensors modeling and propose our model, Hiest. It maintains graph representations from the three perspectives in a meta-learning manner and keeps the hierarchical graph representations in the physical distribution.
- Extensive experimental verifications on three real-world datasets have proven the efficacy of our Hiest against state-of-the-art baselines. Comprehensive analyses have verified the performance of our proposed components.

## 2 PRELIMINARIES

**Definition 2.1. Spatio-Temporal Prediction.** Let  $G = (V, E)$  represent a sensor graph, where  $V$  is the set of  $N$  nodes and  $E$  is the edge set. Each node in the graph represents a traffic sensor in the road network. The topological structure of  $G$  is recorded by the adjacency matrix  $A \in \{0, 1\}^{N \times N}$ , where  $A_{i,j} = 1$  denotes a connection between node  $i$  and  $j$ . Given the historical signal for  $H$  timesteps, spatio-temporal prediction aims to predict the future  $T$  timesteps graph signal:

$$X^{t-H:t}, G \xrightarrow{f_{\theta}} \hat{Y}^{t+1:t+T} \quad (1)$$

where the  $X^{t-H:t} \in \mathbb{R}^{N \times D \times H}$  is historical graph signal and  $\hat{Y}^{t+1:t+T} \in \mathbb{R}^{N \times D \times T}$  is model prediction,  $D$  is feature dimension.

**Definition 2.2 Connected Component (CC).** If  $G'$  is a connected subgraph of  $G$  and is not a part of any larger connected subgraph of  $G$ , then  $G'$  is a Connected Component (CC) of  $G$ .

**Definition 2.3 Cut Vertex.** Node  $v \in V$  is a cut vertex of  $G$  if removing it will increase the number of CC in  $G$ .

**Definition 2.4 Bi-Connected Component (BCC).** If there is no cut vertex in graph  $G$ , then the graph  $G$  will be considered as vertex-biconnected. A vertex-biconnected component is regarded as a Bi-Connected Component (BCC)<sup>2</sup>. For every two nodes from two different BCCs there exists one and only one path, *i.e.*, the path through the cut-vertex connecting the two BCCs.

## 3 FRAMEWORK

### 3.1 Framework Overview

In this section, we detail our proposed framework, Hiest. As shown in Figure 2, our Hiest mainly consists of  $L$  layers of temporal convolution and graph convolution. For temporal information capture, we

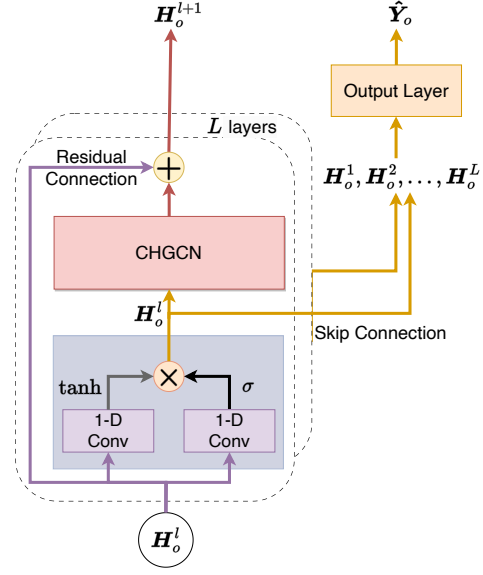


Figure 2: Framework overview of our Hiest.

Table 1: Notation table.

Notation	Definition
$N_o, N_r, N_g$	Number of nodes in the original/regional/global graph
$A_o, A_r, A_g$	Adjacency matrix of the original/regional/global graph
$M_{or}, M_{rg}$	Mapping matrix to indicate the pairwise relationships between the original-regional and regional-global nodes
$H_o, H_r, H_g$	Feature matrix of the original/regional/global graph

introduce 1-D gated casual dilated convolution. To model the complex relationship comprehensively, we elaborate a Cross-Hierarchy Graph Convolutional Network (CHGCN) to capture the proposed regional and global dependency among different nodes. After  $L$  layers representation learning, we concatenate the intermediate representations of each layer and feed the output layer for final prediction. Table 1 denotes the notations for a clear description.

Our CHGCN maintains graph convolution of the original graph, and two proposed hierarchical graphs, *i.e.*, regional and global graphs, as shown in Figure 3, to capture our proposed regional and global dependencies. Moreover, we elaborate a cross-hierarchy information propagation to enhance the spatio-temporal dependency capture in each level and ultimately contribute to the representation learning of the original graph.

### 3.2 Regional Graph Construction

**3.2.1 Motivation.** The original graph describes the pair-wise dependency between nodes. Considering all nodes in an equivalent position in the original structure ignores the hierarchy of the graph. In order to capture the regional perspective of nodes, we propose to merge nodes with close local dependencies into a region. Given the poor connectivity between nodes from different BCCs as in Definition 2.4 and the high local connectivity inside BCC, BCC describes the highly local dependencies in a graph and depicts its intrinsic

<sup>2</sup>In this paper, we denote Bi-Connected Component (BCC) as vertex-biconnected component [36].

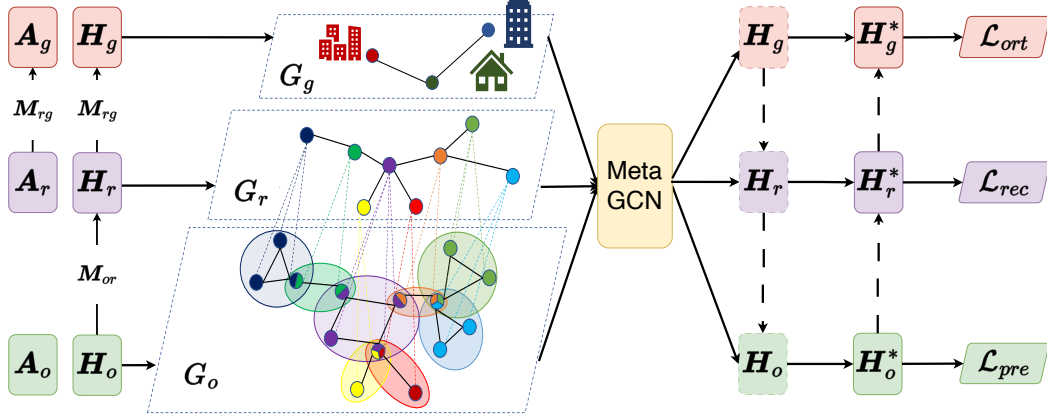


**Figure 3: The pipeline of our CHGCN. Given  $A_o$ ,  $A_r$ , and  $H_o$  as input, we generate  $A_g$  and  $H_g$  by  $M_{rg}$ , and  $H_r$  by  $M_{or}$ . Then we conduct graph convolution by Meta GCN, and update the node representation cross hierarchies.**

structure [36], which accords with our requirement. As shown in Figure 1 (a), node J is a cut-vertex and is the only entry across the BCCs (J,K,L) and (J,M,N). Traffic inside J, K, and L runs mutually, while traffic between J and M is relatively narrow due to the only connection J. So merging BCCs as regional nodes indicates the structure of the sensor graph and describes the macro dependency.

Existing works [7, 28, 29] basically construct the regional nodes by spectral clustering, which do not utilize the topology information and can hardly reflect the skeleton of the road network. The cluster number is also manually assigned, which lacks interpretability. Besides, the hard mapping of clustering, *i.e.*, one node rigorously belongs to one cluster, also hinders the associations of nodes belonging to different clusters, which limits sensor dependency learning.

**3.2.2 Solving Bi-Connected Component.** To better group nodes with high local dependency, we propose a swift solution to describe the regional graph. Specifically, we adapt Tarjan algorithm [25], a classical algorithm based on the Depth-First-Search approach, to solve the BCC given the graph. We construct a regional node in the regional graph  $G_r$  by combining the nodes from the same BCC from the original graph  $G_o$ . The mapping matrix is constructed with the following steps.

Firstly, we establish the mapping matrix  $M_{or} \in \mathbb{R}^{N_o \times N_r}$ , which means the original sensor graph  $G_o$  with  $N_o$  nodes owns  $N_r$  BCCs.  $M_{or}$  indicates if the original node  $i$  is merged to the regional node  $j$  according to the result of Tarjan algorithm. We initialize  $M_{or}[i, j]$  with 1 to represent a mapping between original node  $i$  and regional node  $j$  and 0 otherwise. Then we normalize  $M_{or}$  to keep the sum of each column of  $M_{or}$  equal to 1 and utilize it to generate the feature and adjacency matrix of the regional graph.

In this context, given the feature matrix of the original graph  $H_o \in \mathbb{R}^{N_o \times D}$ , the feature matrix of the regional graph  $H_r \in \mathbb{R}^{N_r \times D}$  will be aggregated according to the mapping matrix  $M_{or}$ ,

$$H_r = M_{or}^T \cdot H_o \quad (2)$$

Meanwhile, given the original graph  $G_o$  with adjacency matrix  $A_o \in \mathbb{R}^{N_o \times N_o}$ , the adjacency matrix of the regional graph  $A_r \in \mathbb{R}^{N_r \times N_r}$  will be generated according to the mapping matrix  $M_{or}$

to maintain the graph connectivity as follows,

$$A_r = M_{or}^T \cdot A_o \cdot M_{or} \quad (3)$$

With the idea that original nodes with high dependency should be mapped together into regional nodes, we can use their representation to reconstruct the original graph. To facilitate the graph representation learning of  $G_r$ , we deploy a binary cross-entropy function [29] to compute the reconstruction loss  $\mathcal{L}_{rec,ro}$  from the regional graph to the original graph  $G_o$ . We use the representation of the regional nodes to reconstruct the adjacency matrix of the original graph as follows,

$$\hat{H}_o = M_{or}^T \cdot H_r \quad (4)$$

$$\hat{A}_o = \text{sigmoid}(\hat{H}_o \cdot \hat{H}_o^T) \quad (5)$$

where the sigmoid function transforms the value between 0 and 1.

Then the reconstruction loss from regional to original graph  $\mathcal{L}_{rec,ro}$  is constructed as follows,

$$\begin{aligned} \mathcal{L}_{rec,ro} = & \frac{1}{N_o^2} \sum_{i,j \in V_o} -A_o[i, j] \log(\hat{A}_o[i, j]) \\ & - (1 - A_o[i, j]) \log(1 - \hat{A}_o[i, j]) \end{aligned} \quad (6)$$

where  $V_o$  is the vertex set of the original graph  $G_o$ .

Through this combination, we can easily capture the high local dependency on topology information and avoid deciding the cluster number. Our solution achieves this goal effectively with linear time complexity of  $O(|V| + |E|)$ . Furthermore, we repetitively assign the cut-vertex to the regional node corresponding to the BCC it belongs to, since it acts as a hub connecting multiple communities. The mapping matrix  $M_{or}$  is calculated offline and needs no update, which enjoys superior computational and maintenance costs.

### 3.3 Global Graph Construction

**3.3.1 Motivation.** The regions with similar properties, such as functions or population density, usually have common spatial-temporal patterns that are different from those with different properties. For example, the rush hour of the living areas is usually similar to each other, while different from the CBD areas. Such common and

representative spatio-temporal patterns across the city can offer auxiliary information to spatio-temporal representation learning of the original graph as a global dependency. The ideal situation is that some auxiliary data, *e.g.*, POI data, can be utilized to indicate the functionality of regions, *i.e.*, describes the global dependency explicitly. However, this is often not the case, and manually defining the common regions always lacks generality and demands tremendous expert effort. To achieve the common spatio-temporal patterns across the city, we build a global view of the graph  $G_g$ , consisting of nodes with the most representative spatio-temporal patterns.

**3.3.2 Generating Common Nodes.** In this section, we generate common and representative spatio-temporal representations given the regional graph  $G_r$ . Basically, we utilize a trainable soft-mapping matrix to generate the global nodes. Furthermore, we integrate the orthogonal constraint to pursue the global representations to be different from each other.

We set mapping matrix  $M_{rg} \in \mathbb{R}^{N_r \times N_g}$  to indicate the mapping between nodes in  $G_r$  and  $G_g$ . It is noteworthy that  $M_{rg}$  is trainable according to model optimization. Given the adjacency matrix of the regional graph  $A_r \in \mathbb{R}^{N_r \times N_r}$ , the adjacency matrix of the global graph  $A_g \in \mathbb{R}^{N_g \times N_g}$  is generated as follows,

$$A_g = M_{rg}^T \cdot A_r \cdot M_{rg} \quad (7)$$

Similarly, given the feature matrix of the regional graph  $H_r \in \mathbb{R}^{N_r \times D}$ , the feature matrix of the global graph  $X_g \in \mathbb{R}^{N_g \times D}$  is generated as follows,

$$H_g = M_{rg}^T \cdot H_r \quad (8)$$

To keep representative spatio-temporal patterns in  $G_g$ , we integrate orthogonal loss to diversify the nodes' representations. We minimize the cosine similarity of every two nodes in  $G_g$ ,

$$\mathcal{L}_{ort} = \frac{1}{C_{N_g}^2} \sum_{i=1}^{N_g} \sum_{j=i+1}^{N_g} \left| \frac{H_g[i] \odot H_g[j]}{\|H_g[i]\| \|H_g[j]\|} \right| \quad (9)$$

where  $C_{N_g}^2$  is the number of 2-combinations of  $N_g$ . Similarly, to enhance the graph representation learning, we incorporate reconstruction loss as in Equation (6) to reconstruct the regional graph  $G_r$  from the global graph  $G_g$ ,

$$\mathcal{L}_{rec_{gr}} = \frac{1}{N_r^2} \sum_{i,j \in V_r} -A_r[i,j] \log(\hat{A}_r[i,j]) - (1 - A_r[i,j]) \log(1 - \hat{A}_r[i,j]) \quad (10)$$

where  $V_r$  is the vertex set of the regional graph  $G_r$ .

It is worth notation that our trainable  $M_{rg}$  implements a soft mapping from regional nodes to global nodes, which is in line with the fact that each region can represent diverse properties. Hence, our global nodes can serve as base vectors to describe any sensor considering the spatio-temporal patterns to contain the representative and common patterns of physical sensors.

### 3.4 Hierarchical Graph Convolution

**3.4.1 Meta Graph Convolution.** To capture the spatial dependencies on the given graph and describe the nodes in the two hierarchical graphs in the physical data space, we introduce a Meta GCN

to generate their graph signals. We incorporate diffusion convolution [16], which is proven to be effective and calculated efficiently in spatial modeling, to capture the spatial dependency.

We use a Meta GCN to process representation learning of  $G_o$ ,  $G_r$ , and  $G_g$ , in order to describe nodes in three levels in the same data distribution. By projecting the regional and global nodes to the data space of physical sensors, we can generate nodes of hierarchical levels with reality and generality.

Specifically, take the original graph  $G_o$  as an example, given Graph  $G_o$  and the adjacency matrix  $A_o \in \mathbb{R}^{N_o \times N_o}$  and input feature matrix  $H_o \in \mathbb{R}^{N_o \times D}$  of it, the general output  $H_o \in \mathbb{R}^{N_o \times D}$  of graph convolution [14] can be formulated as follows,

$$H_o = A_o H_o W \quad (11)$$

where  $W \in \mathbb{R}^{D \times D}$  is the trainable parameter matrix. The graph convolution is the same for  $G_r$  and  $G_g$ .

**3.4.2 Hierarchical Information Enhanced Representation Learning.** With the three hierarchical graphs, we are able to maintain the dependency of nodes at three different levels. We propose hierarchical graph convolution to enhance representation learning with hierarchical graph information.

After processing by Meta GCN, we attain the updated representations of the three layers as  $H_o$ ,  $H_r$ , and  $H_g$ , respectively. In order to strengthen the information propagation between different levels, we first enhance the node representation from top to bottom and then update backward, as shown in the dashed lines in Figure 3. Next, we introduce the cross-hierarchy representation learning of two steps, *i.e.*, the enhancement of  $H_o^*$  to integrate the information from common and regional hierarchies, and the representation update of  $H_r^*$  and  $H_g^*$ .

To enhance the representation of the nodes in the original graph, we sequentially propagate the common information to the regional representation  $H_r$ , and then the enhanced representation of the original graph  $H_o^*$  can be calculated as,

$$H_r = H_r + \eta_1 \cdot \sigma(M_{rg} \cdot H_g) \quad (12)$$

$$H_o^* = H_o + \eta_2 \cdot \sigma(M_{or} \cdot H_r) \quad (13)$$

where  $\sigma$  is the Relu activation function,  $M_{or}$  and  $M_{rg}$  is the mapping matrix.  $\eta_1$  and  $\eta_2$  are the hyperparameters to control the enhancement ratio.

As the representation of the original graph is enhanced, we also update the representation of regional and global graphs in reverse. We design the update process to propagate the node representation from the lower levels to higher levels and attain the node representation of regional graph  $H_r^*$  and global graph  $H_g^*$ , respectively,

$$H_r^* = H_r + \eta_3 \cdot \sigma(M_{or}^T \cdot H_o^*) \quad (14)$$

$$H_g^* = H_g + \eta_4 \cdot \sigma(M_{rg}^T \cdot H_r^*) \quad (15)$$

where  $M_{or}^T$  and  $M_{rg}^T$  is the transverse of the mapping matrix  $M_{or}$  and  $M_{rg}$ .  $\eta_3$  and  $\eta_4$  are hyperparameters to control the update ratio.

### 3.5 Temporal Dependency Learning

For the temporal dependency learning, we incorporate the 1-D casual dilated convolution with gate mechanism, named TCN [35].

Given the input feature matrix of the original graph  $H_o \in \mathbb{R}^{N \times D}$ , the output of the gated TCN can be presented as follows,

$$H_o = \tanh(\theta_1 \star H_o + b_1) \odot \sigma(\theta_2 \star H_o + b_2) \quad (16)$$

where  $\sigma$  is the sigmoid function,  $\odot$  is the element-wise production,  $\theta_1, \theta_2, b_1, b_2$  are the model parameters.

### 3.6 Optimization

The optimization objective function of our model contains four parts, the prediction loss  $\mathcal{L}_{pre}$ , the reconstruction loss from regional to original graph  $\mathcal{L}_{rec_{ro}}$ , the reconstruction loss from global to regional graph  $\mathcal{L}_{rec_{gr}}$  and the orthogonal loss  $\mathcal{L}_{ort}$ . We deploy the MAE to evaluate the difference between the prediction and the ground truth as the prediction loss  $\mathcal{L}_{pre}$  as follows,

$$\mathcal{L}_{pre} = \frac{1}{TN_o} \sum_{i=1}^T \sum_{j=1}^{N_o} |\hat{Y}_j^i - Y_j^i| \quad (17)$$

Hence the complete optimization objective function is,

$$\mathcal{L} = \mathcal{L}_{pre} + \mathcal{L}_{rec_{ro}} + \mathcal{L}_{rec_{gr}} + \mathcal{L}_{ort} \quad (18)$$

## 4 EXPERIMENT

### 4.1 Datasets

The datasets used in this paper can be found in the public repos. METR\_LA and PEMS\_BAY traffic speed datasets are released by Li *et al.* [16] and PEMS\_D8 traffic flow datasets are released by Yan *et al.* [32]. Each vertex on the graph represents a sensor to collect the traffic flow/speed data. The summary statistics of the key elements of the datasets are shown in Table 2. Our graph construction follows the general setting [24]. We constructed the adjacency matrix using distances between sensors with a threshold Gaussian kernel. We set the threshold to 0.1 for all datasets.

### 4.2 Baselines

We compare our proposed HIEST against the following baseline models on spatial-temporal prediction tasks. The baseline models can be divided into three main categories depending on how they process the given Graph. The first category considers the graph as a fixed, completed graph, such as DCRNN [16], GMAN [45], STGCN [34], and TGCN [40]. The second category considers the graph as incomplete and learns potential links, such as GWnet [31], GTS [23], and MTGNN [30]. The third category aims to extract hierarchical information from the given graph, including HGCN [29] and Trans [32].

- SVR: A ML regression method for time series prediction.
- DCRNN: Diffusion graph convolutional networks applied as the spatial feature extractor and RNN as the temporal feature extractor to extract spatial-temporal correlations.
- STGCN: STGCN integrates graph convolution and gated time convolution to capture spatio-temporal correlations.
- GraphWavenet (GWnet): Casual Dialated Convolution for extracting the temporal features. Diffusion convolution is adapted for the graph convolution layer of GraphWavenet.
- TGCN: TGCN combines the GCN and GRU for spatial-temporal predicting.

**Table 2: Datasets statistics.**

Dataset	#Nodes	#Edges	#Timesteps	Period
PEMS_BAY	325	2,369	34,272	2017/01/01 - 2017/06/30
PEMS_D8	170	276	17,856	2016/07/01 - 2016/08/31
METR_LA	207	1,515	52,116	2012/03/01 - 2012/06/27

- GMAN: GMAN applies attention mechanism to extract spatial and temporal features for prediction.
- MTGNN: MTGNN can model potential spatial dependencies between pairs of variables in multivariate time series data.
- GTS: GTS proposes learning the graph structure simultaneously with the GNN if the graph is unknown.
- HGCN: HGCN is a hierarchical-based ST prediction model with spectral clustering.
- Traffic-Transformer (Trans): Trans proposes a hierarchical-based Transformer with a global encoder and global-local decoder to extract and fuse the spatial-temporal patterns globally and locally.

### 4.3 Experiments Setups

We split the data into training, validation, and testing sets with a ratio of 7:1:2 for all datasets. The hidden size is 32. The number of blocks and layers is 4 and 2, respectively. We predict the spatio-temporal attributes *i.e.*, traffic speed or flow, of the future 12 timesteps based on the historical 12 timesteps, *i.e.*,  $T = H = 12$ . For the hyperparameters of our proposed HIEST, we set  $\eta_1, \eta_2, \eta_3, \eta_4 = 1$  and  $N_g = 15$  for all datasets.

To comprehensively evaluate the methods, we present the performance of mean absolute error **MAE**, mean absolute percentage error **MAPE**, and root mean squared error **RMSE**. To ensure a fair comparison between our HIEST and the baselines, we refer to the public repository LibCity [27]. All experiments are executed on 1 NVIDIA V100s with the random seed set to 0 and repeated thrice.

### 4.4 Overall Performance

The overall results over 3 real-world datasets are shown in Table 3. From the performance comparison against state-of-the-art baselines, several conclusions can be made:

HIEST consistently outperforms DCRNN, GMAN, STGCN, and TGCN. These baseline models consider the sensors equally without any hierarchical information capture. In contrast, our proposed HIEST uses a regional and global graph to describe the macro-structure of the original sensor graph and capture implicit higher-order neighborhood relations. This enables HGCN to handle spatio-temporal representation learning comprehensively.

GWnet, GTS, and MTGNN propose to model the intrinsic relationship among nodes by establishing trainable adjacency matrices or optimizing a probabilistic graph model. Dense data with plenty of sensors can foster their proposed intrinsic dependency modeling. Our proposed method achieves competitive performance against them with only 48% of the parameters used by MTGNN and 0.5%-0.7% of GTS. On the PEMS\_D8 dataset with fewer nodes, edges, and recordings, our proposed HIEST outperforms them by utilizing

**Table 3: Overall performance comparison. Best performances are bold, next best are underlined.**

Dataset	Model	15 min			30 min			60 min			Params(K)
		MAE	MAPE	RMSE	MAE	MAPE	RMSE	MAE	MAPE	RMSE	
METR_LA	SVR	4.23	9.46%	9.97	5.28	11.71%	12.27	7.00	15.59%	15.33	-
	DCRNN	2.55	6.54%	5.08	3.02	8.27%	6.29	3.57	10.40%	7.60	372
	STGCN	2.76	7.13%	5.10	3.43	9.61%	6.60	4.31	12.62%	8.26	320
	GWnet	2.55	6.67%	5.19	2.96	8.11%	6.26	3.39	9.57%	7.29	276
	TGCN	3.11	8.22%	5.42	3.63	9.97%	6.39	4.30	12.17%	7.46	32
	GMAN	2.85	7.56%	5.17	3.27	9.08%	<u>6.10</u>	3.72	10.68%	<b>7.00</b>	900
	MTGNN	2.49	<u>6.31%</u>	5.03	<u>2.91</u>	<u>7.91%</u>	6.12	3.38	<b>9.54%</b>	7.24	405
	GTS	<u>2.48</u>	6.35%	<u>5.01</u>	<u>2.91</u>	7.96%	6.13	3.40	9.90%	7.35	38,494
	HGCN	2.59	6.70%	5.17	3.06	8.45%	6.35	3.60	10.40%	7.55	690
	Trans	2.68	6.97%	5.33	3.11	8.54%	6.50	3.58	10.13%	7.62	220
	<b>HIEST</b>	<b>2.46</b>	<b>6.19%</b>	<b>4.91</b>	<b>2.89</b>	<b>7.76%</b>	<b>6.02</b>	<b>3.37</b>	<b>9.54%</b>	<u>7.16</u>	275
PEMS_BAY	SVR	1.61	3.87%	3.58	2.00	4.76%	4.58	2.69	6.44%	6.20	-
	DCRNN	<u>1.32</u>	2.74%	<u>2.78</u>	1.66	3.70%	3.79	2.07	4.64%	4.64	372
	STGCN	1.38	2.89%	2.83	1.82	4.07%	3.99	2.37	5.32%	5.12	320
	GWnet	<u>1.32</u>	2.77%	2.79	1.65	3.71%	3.74	1.98	4.59%	4.54	279
	TGCN	1.60	3.36%	3.02	2.00	4.44%	3.99	2.53	5.79%	4.95	32
	GMAN	1.51	3.21%	2.97	1.82	4.06%	3.86	2.10	4.79%	4.53	900
	MTGNN	<u>1.32</u>	2.77%	<u>2.78</u>	1.64	3.64%	<u>3.71</u>	1.94	<b>4.41%</b>	4.47	573
	GTS	<b>1.30</b>	<u>2.70%</u>	<u>2.78</u>	<b>1.61</b>	<b>3.58%</b>	<u>3.71</u>	<b>1.90</b>	<u>4.43%</u>	<u>4.45</u>	58,462
	HGCN	1.35	2.88%	2.85	1.70	3.91%	3.85	2.03	4.84%	4.62	766
	Trans	1.40	2.96%	2.89	1.71	3.77%	3.81	2.04	4.58%	4.65	220
	<b>HIEST</b>	<b>1.30</b>	<b>2.69%</b>	<b>2.74</b>	<u>1.63</u>	<u>3.63%</u>	<b>3.68</b>	<u>1.93</u>	4.50%	<b>4.44</b>	275
PEMS_D8	SVR	93.08	66.81	120.29	93.01	67.12	120.36	92.92	67.78	120.59	-
	DCRNN	15.13	9.82%	23.48	16.66	10.79%	26.09	19.43	12.51%	30.32	372
	STGCN	14.95	9.63%	23.24	16.85	10.87%	26.13	20.17	12.84%	30.91	296
	GWnet	14.49	9.66%	22.89	15.76	11.05%	25.14	18.17	12.46%	28.84	289
	TGCN	16.68	12.82%	25.18	18.00	13.70%	27.28	21.19	16.58%	31.67	32
	GMAN	14.37	10.27%	22.85	15.23	10.75%	24.51	17.00	12.09%	27.02	900
	MTGNN	13.94	9.02%	22.04	14.84	<u>9.53%</u>	23.76	16.65	10.90%	<u>26.35</u>	352
	GTS	<u>13.62</u>	<u>8.81%</u>	<u>21.84</u>	<u>14.59</u>	<u>9.53%</u>	<u>23.68</u>	<u>16.26</u>	<u>10.79%</u>	26.43	20,164
	HGCN	15.44	10.58%	26.30	16.91	11.88%	26.39	19.87	14.97%	30.43	671
	Trans	17.78	13.02%	26.94	19.02	13.89%	28.98	22.34	16.10%	33.93	220
	<b>HIEST</b>	<b>13.42</b>	<b>8.62%</b>	<b>21.66</b>	<b>14.23</b>	<b>9.31%</b>	<b>23.50</b>	<b>15.64</b>	<b>10.23%</b>	<b>25.97</b>	275

the proposed global graph nodes, whose universal and representative spatio-temporal representation is guaranteed by orthogonal constraints of CHGCN.

Next, we discuss the two hierarchical spatio-temporal prediction baselines. Hiest outperforms HGCN on all settings. HGCN conducts a new hierarchy above the original graph by spectral clustering, while our proposed method conducts new hierarchies from two perspectives: the regional and global graphs described in the real data space. The better results of Hiest over HGCN demonstrate the superiority of our proposed two new hierarchies over the simple hierarchy in HGCN.

Hiest also outperforms Trans on all three datasets. Trans proposes a global encoder with a multi-head attention block to capture common global spatial-temporal patterns, ignoring the topological structure of the graph. It masks the attention matrix based on the high-order adjacency matrix to incorporate hierarchical neighbor information. In contrast, our solver for BCCs requires linear computational complexity and enjoys promising interpretability considering the topology structure.

Hiest achieves competitive performance against the state-of-the-art baselines across all horizons, which demonstrates its ability for both short-term and long-term prediction. Its two hierarchical graphs capture the macro dependency and common properties of sensors, and the cross-hierarchy graph convolution network well enhances the information propagation among different levels, then contributes to the spatio-temporal dependency learning of sensors.

#### 4.5 Ablation Study

The two most critical components of our Hiest are the two new hierarchies, *i.e.*, regional and global perspectives, and the cross-hierarchy representation learning consisting of enhance process and update process. To verify their effectiveness explicitly, we generated the following variations of our model:

- *w/o EU*: Hiest without the enhance and update process across all three layers.
- *w/o U*: Hiest without the update of  $H_r^*$  and  $H_g^*$ .

**Table 4: Ablation study results.**

Model	15 min			30 min			60 min		
	MAE	MAPE	RMSE	MAE	MAPE	RMSE	MAE	MAPE	RMSE
<i>w/o EU</i>	14.31	9.09%	22.84	15.57	10.02%	25.20	17.79	11.51%	28.89
<i>w/o U</i>	<u>13.73</u>	<u>9.05%</u>	<u>22.17</u>	<u>14.68</u>	9.66%	<u>23.97</u>	<u>16.32</u>	<u>10.59%</u>	<u>26.47</u>
<i>w/o G<sub>g</sub></i>	14.02	9.23%	22.41	14.90	<u>9.57%</u>	24.32	16.80	11.08%	27.54
<i>w/o G<sub>r</sub></i>	14.95	9.63%	23.24	16.85	10.87%	26.13	20.17	12.84%	30.91
<b>HIEST</b>	<b>13.42</b>	<b>8.62%</b>	<b>21.66</b>	<b>14.23</b>	<b>9.31%</b>	<b>23.50</b>	<b>15.64</b>	<b>10.23%</b>	<b>25.97</b>

**Table 5: Parameter analysis results for  $\eta_4$ .**

$\eta_4$	15 min			30 min			60 min		
	MAE	MAPE	RMSE	MAE	MAPE	RMSE	MAE	MAPE	RMSE
0	<u>13.63</u>	9.04%	<u>21.88</u>	14.50	9.48%	<u>23.63</u>	16.08	10.46%	26.27
0.2	13.65	8.94%	21.92	14.52	9.52%	23.76	16.05	10.49%	26.23
0.5	13.64	8.84%	<u>21.88</u>	<u>14.49</u>	9.45%	23.71	<u>15.94</u>	<u>10.39%</u>	<u>26.17</u>
0.8	13.71	<u>8.80%</u>	22.01	14.66	<u>9.40%</u>	24.09	16.24	10.62%	26.61
1	<b>13.42</b>	<b>8.62%</b>	<b>21.66</b>	<b>14.23</b>	<b>9.31%</b>	<b>23.50</b>	<b>15.64</b>	<b>10.23%</b>	<b>25.97</b>

- *w/o G<sub>g</sub>*: HIEST without the global graph, *i.e.*, consisting of original graph  $G_o$  and  $G_r$ .
- *w/o G<sub>r</sub>*: HIEST without the regional graph, *i.e.*, consisting of original graph  $G_o$  and  $G_g$ .

Table 4 presents the results of the ablation study. We can draw a conclusion that both the two proposed hierarchies and the enhanced information are critical to our proposed model. The superiority of HIEST over *w/o EU* proves that our proposed hierarchical update mechanism and generic nodes can foster the learning of the spatio-temporal representation of the original graph. The results of *w/o U* demonstrate that the information propagation from lower layers to higher ones can also benefit spatio-temporal dependency capture, which emphasizes the efficacy of our cross-hierarchy representation learning. The results of *w/o G<sub>g</sub>* indicate that our generated common representation offers essential information to the original sensor graph modeling. *w/o G<sub>r</sub>* achieves poor results without the regional graph describing the macro dependency. The global graph can not be well constructed directly over the sensor-level, which proves the validity of our two progressively hierarchical perspectives.

#### 4.6 Hyperparameter Analysis

To further verify the efficacy of our proposed global graph and the update process from the regional graph to the global graph, with  $\eta_1, \eta_2, \eta_3 = 1$ , we conduct the analysis for the hyperparameters,  $N_g \in \{10, 15, 20, 25\}$  and  $\eta_4 \in \{0, 0.2, 0.5, 0.8, 1\}$ , of our proposed model HIEST on the PEMS\_D8 datasets:

Table 5 presents the results of applying different update ratios  $\eta_4$ , and those less than 1 indicate that the updated regional representation should be given equal importance to provide comprehensive information when updating the global representation. Otherwise, it can be considered as noise that contradicts the good mapping between the regional and global graphs.

Table 6 shows that different numbers of global nodes  $N_g$  lead to comparable results, which are generally better than baselines.

**Table 6: Parameter analysis results for  $N_g$ .**

$N_g$	15 min			30 min			60 min		
	MAE	MAPE	RMSE	MAE	MAPE	RMSE	MAE	MAPE	RMSE
10	13.54	<u>8.76%</u>	21.79	14.43	9.44%	23.62	15.96	10.57%	26.21
15	<b>13.42</b>	<b>8.62%</b>	<b>21.66</b>	<b>14.23</b>	<b>9.31%</b>	<u>23.50</u>	<u>15.64</u>	<u>10.23%</u>	<u>25.97</u>
20	13.50	9.14%	21.77	14.42	9.97%	23.67	15.82	10.38%	26.15
25	<u>13.47</u>	9.04%	<u>21.74</u>	<u>14.26</u>	9.49%	<b>23.47</b>	<b>15.59</b>	<b>10.08%</b>	<b>25.72</b>

Our proposed model is not very sensitive to the number of global nodes, and both dense or sparse base vectors can well describe the vector space of sensors spatio-temporal patterns.

#### 4.7 Visualization

To achieve a close view of our HIEST, we visualize the two hierarchical graphs  $G_r$  and  $G_g$  on METR\_LA, as shown in Figure 4. Specifically, we color original nodes with their related regions as Figure 4 (a). The 207 sensors in  $G_o$  are divided into 136 regions in  $G_r$ , and we color using 10 colors according to the constraint that any two adjacent nodes from different regions are within different colors. For Figure 4 (b), we illustrate the common and representative properties of regions and mark the POIs near sensors. We generate 15 global nodes, *i.e.*, 15 colors, to depict which global node the sensor belongs to. Notably, considering that each region is assigned a weight vector of all global nodes in the soft-mapping matrix  $M_{rg}$ , we choose the global node with the highest weight for illustration.

For the mapping results from the regional perspective in Figure 4 (a), it is in accordance with the expectation that the regional node depicts region properties to some extent. We zoom in on two areas of the blue and orange rectangles. In the orange rectangle, many pink sensors report traffic conditions of a huge residential area. So it is conceivable that they are grouped into one region. Furthermore, the red sensors are grouped into another region because they are in different directions of the same road, and are supposed to report different states. In the blue rectangle, the brown sensors are identified to be highly-related due to they belong to the same community. Besides, as the road goes to the mount area, the yellow sensors are recognized as another region. These illustrations reflect the macro dependency captured of our regional graph, which utilizes the topology information and accords to the physical meaning.

In terms of the global perspective in Figure 4 (b), we can observe that sensors in the same color have POI of similar functions as neighbors. There are consistently schools in the vicinity of the dark blue sensors, as shown in the magnified rectangles, reflecting the highly similar spatio-temporal patterns of these sensors. Also, the pink sensor always appears with recreational POIs, such as nature parks or theme parks, which implies that HIEST successfully identifies the function in the region where the sensor is located. Notably, the mapping between regional and global graphs is soft, which means this observation may be a partial factor of the complex spatio-temporal patterns. However, we can still safely draw a conclusion that the common spatio-temporal patterns we mined can explain the properties of regions, which can provide auxiliary information for sensor modeling.

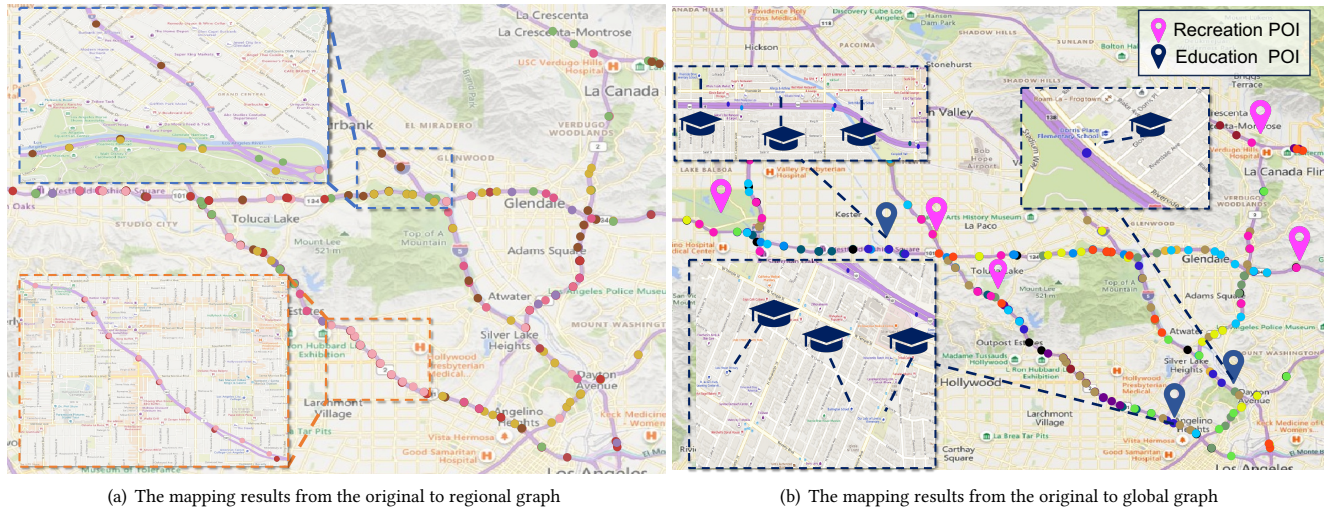


Figure 4: The visualization on METR\_LA.

## 5 RELATED WORKS

**Spatio-Temporal Prediction.** Spatio-temporal prediction involves predicting future trends by analyzing historical spatio-temporal properties. Early approaches [9, 15, 37, 38] were based on grid-based data, where the city is divided into grids, and Convolutional Neural Networks (CNN) are used to capture spatial dependencies between a grid and its neighbors. These approaches generally incorporate TCN [35] and RNN [21] to capture temporal variations. For the later works [16, 31, 39] on graph-based data, Graph Neural Networks (GNN) are applied under the assumption that connected sensors in the graph have similar patterns within the same period.

Basically, these approaches treat every sensor equally and overlook the implicit hierarchical structures present in the original graph. With our HIEST, the inherent hierarchy can be used to enhance the representation of the original sensor graph.

**Hierarchical Spatio-Temporal Data Mining.** Existing hierarchical spatio-temporal data mining works implement hierarchy construction by clustering node representations [7, 17, 18, 28, 29, 32]. Traffic-Transformer [32] and ST-HSL [17] capture global node dependencies using multi-head attention mechanisms and hypergraphs. HGNN [29] and HiGCN [18] generate new hierarchies using unique trainable GAT or GCN models, while MC-STGCN [28] uses the Louvain algorithm [4] to detect potential communities.

Some works [7, 28, 29] attempt to build an implicit hierarchy in the graph’s topological structure using spectral clustering [22] but achieve suboptimal performance. Instead, our method efficiently solves the BCC to merge sensors with high intra-region dependency and generate the regional map with linear time complexity, which does not require updating or training and can be easily extended. Other works [18, 29] construct unique graph neural networks for different hierarchies. In contrast, we incorporate a Meta GCN. By decoupling complex associations between sensors, we extract two hierarchical perspectives, which yields a comprehensive view of spatio-temporal representation learning.

## 6 CONCLUSION

The key to solving spatio-temporal prediction is how to model the dependency among all sensors. Basically, existing models simply regard all nodes in an equal position, or devise a hierarchy based on simply clustering. In this paper, we rethink the sensor’s dependency modeling and propose our HIEST, to enhance spatio-temporal prediction with hierarchical information effectively. We propose two hierarchical perspectives, *i.e.*, regional and global graphs, to describe the macro dependency among sensors and generate representative and common spatio-temporal patterns. Furthermore, we elaborate the cross-hierarchy graph learning mechanism, CHGCN, to learn node representation in a meta-learning manner and facilitate information propagation among nodes in multiple levels.

## ACKNOWLEDGMENTS

This research was partially supported by APRC - CityU New Research Initiatives (No.9610565, Start-up Grant for New Faculty of City University of Hong Kong), CityU - HKIDS Early Career Research Grant (No.9360163), Hong Kong ITC Innovation and Technology Fund Midstream Research Programme for Universities Project (No.ITS/034/22MS), SIRG - CityU Strategic Interdisciplinary Research Grant (No.7020046, No.7020074), SRG-Fd - CityU Strategic Research Grant (No.7005894), Tencent (CCF-Tencent Open Fund, Tencent Rhino-Bird Focused Research Fund), Huawei (Huawei Innovation Research Program), Ant Group (CCF-Ant Research Fund, Ant Group Research Fund) and Kuaishou. Hongwei Zhao is funded by the Provincial Science and Technology Innovation Special Fund Project of Jilin Province, grant number 20190302026GX, Natural Science Foundation of Jilin Province, grant number 20200201037JC, and the Fundamental Research Funds for the Central Universities, JLU. Zitao Liu is supported by National Key R&D Program of China, under Grant No. 2022YFC3303600, and Key Laboratory of Smart Education of Guangdong Higher Education Institutes, Jinan University (2022LSYS003).

## REFERENCES

- [1] Di Chai, Leye Wang, and Qiang Yang. 2018. Bike flow prediction with multi-graph convolutional networks. In *Proceedings of the 26th ACM SIGSPATIAL international conference on advances in geographic information systems*. 397–400.
- [2] Cen Chen, Kenli Li, Sin G Teo, Xiaofeng Zou, Kang Wang, Jie Wang, and Zeng Zeng. 2019. Gated residual recurrent graph neural networks for traffic prediction. In *Proceedings of the AAAI conference on artificial intelligence*, Vol. 33. 485–492.
- [3] Weiqi Chen, Ling Chen, Yu Xie, Wei Cao, Yusong Gao, and Xiaojie Feng. 2020. Multi-range attentive bicomponent graph convolutional network for traffic forecasting. In *Proceedings of the AAAI conference on artificial intelligence*, Vol. 34. 3529–3536.
- [4] Pasquale De Meo, Emilio Ferrara, Giacomo Fiumara, and Alessandro Proveti. 2011. Generalized louvain method for community detection in large networks. In *2011 11th international conference on intelligent systems design and applications*. IEEE, 88–93.
- [5] Dingxiong Deng, Cyrus Shahabi, Ugur Demiryurek, Linhong Zhu, Rose Yu, and Yan Liu. 2016. Latent space model for road networks to predict time-varying traffic. In *Proceedings of the 22nd ACM SIGKDD international conference on knowledge discovery and data mining*. 1525–1534.
- [6] Zulong Diao, Dafang Zhang, Xin Wang, Kun Xie, Shaoyao He, Xin Lu, and Yanbiao Li. 2018. A hybrid model for short-term traffic volume prediction in massive transportation systems. *IEEE Transactions on Intelligent Transportation Systems* 20, 3 (2018), 935–946.
- [7] Kan Guo, Yongli Hu, Yanfeng Sun, Sean Qian, Junbin Gao, and Bao cai Yin. 2021. Hierarchical graph convolution network for traffic forecasting. In *Proceedings of the AAAI conference on artificial intelligence*, Vol. 35. 151–159.
- [8] Shengnan Guo, Youfang Lin, Ning Feng, Chao Song, and Huaiyu Wan. 2019. Attention based spatial-temporal graph convolutional networks for traffic flow forecasting. In *Proceedings of the AAAI conference on artificial intelligence*, Vol. 33. 922–929.
- [9] Shengnan Guo, Youfang Lin, Shijie Li, Zhaoming Chen, and Huaiyu Wan. 2019. Deep spatial-temporal 3D convolutional neural networks for traffic data forecasting. *IEEE Transactions on Intelligent Transportation Systems* 20, 10 (2019), 3913–3926.
- [10] Liangzhe Han, Bowen Du, Leilei Sun, Yanjie Fu, Yisheng Lv, and Hui Xiong. 2021. Dynamic and multi-faceted spatio-temporal deep learning for traffic speed forecasting. In *Proceedings of the 27th ACM SIGKDD conference on knowledge discovery & data mining*. 547–555.
- [11] Xiao Han, Xiangyu Zhao, Liang Zhang, and Wanyu Wang. 2023. Mitigating Action Hysteresis in Traffic Signal Control with Traffic Predictive Reinforcement Learning. 673–684.
- [12] Peilan He, Guiyuan Jiang, Siew-Kei Lam, and Dehua Tang. 2018. Travel-time prediction of bus journey with multiple bus trips. *IEEE Transactions on Intelligent Transportation Systems* 20, 11 (2018), 4192–4205.
- [13] Wei Jin, Xiaorui Liu, Xiangyu Zhao, Yao Ma, Neil Shah, and Jiliang Tang. 2022. Automated Self-Supervised Learning for Graphs. In *10th International Conference on Learning Representations (ICLR 2022)*.
- [14] Thomas N Kipf and Max Welling. 2016. Semi-supervised classification with graph convolutional networks. *arXiv preprint arXiv:1609.02907* (2016).
- [15] Ting Li, Junbo Zhang, Kainan Bao, Yuxuan Liang, Yexin Li, and Yu Zheng. 2020. Autost: Efficient neural architecture search for spatio-temporal prediction. In *Proceedings of the 26th ACM SIGKDD International Conference on Knowledge Discovery & Data Mining*. 794–802.
- [16] Yaguang Li, Rose Yu, Cyrus Shahabi, and Yan Liu. 2018. Diffusion Convolutional Recurrent Neural Network: Data-Driven Traffic Forecasting. In *International Conference on Learning Representations (ICLR '18)*.
- [17] Zhonghang Li, Chao Huang, Lianghao Xia, Yong Xu, and Jian Pei. 2022. Spatial-Temporal Hypergraph Self-Supervised Learning for Crime Prediction. In *2022 IEEE 38th International Conference on Data Engineering (ICDE)*. IEEE, 2984–2996.
- [18] Yihong Ma, Patrick Gerard, Yijun Tian, Zhichun Guo, and Nitesh V Chawla. 2022. Hierarchical Spatio-Temporal Graph Neural Networks for Pandemic Forecasting. In *Proceedings of the 31st ACM International Conference on Information & Knowledge Management*. 1481–1490.
- [19] Haitao Mao, Zhikai Chen, Wei Jin, Haoyu Han, Yao Ma, Tong Zhao, Neil Shah, and Jiliang Tang. 2023. Demystifying Structural Disparity in Graph Neural Networks: Can One Size Fit All? *arXiv preprint arXiv:2306.01323* (2023).
- [20] Haitao Mao, Lun Du, Yujia Zheng, Qiang Fu, Zelin Li, Xu Chen, Shi Han, and Dongmei Zhang. 2021. Source free unsupervised graph domain adaptation. *arXiv preprint arXiv:2112.00955* (2021).
- [21] Larry R Medsker and LC Jain. 2001. Recurrent neural networks. *Design and Applications* 5 (2001), 64–67.
- [22] Andrew Ng, Michael Jordan, and Yair Weiss. 2001. On spectral clustering: Analysis and an algorithm. *Advances in neural information processing systems* 14 (2001).
- [23] Chao Shang and Jie Chen. 2021. Discrete Graph Structure Learning for Forecasting Multiple Time Series. In *Proceedings of International Conference on Learning Representations*.
- [24] David I Shuman, Sunil K Narang, Pascal Frossard, Antonio Ortega, and Pierre Vandergheynst. 2013. The emerging field of signal processing on graphs: Extending high-dimensional data analysis to networks and other irregular domains. *IEEE signal processing magazine* 30, 3 (2013), 83–98.
- [25] Robert Tarjan. 1972. Depth-first search and linear graph algorithms. *SIAM journal on computing* 1, 2 (1972), 146–160.
- [26] Dong Wang, Junbo Zhang, Wei Cao, Jian Li, and Yu Zheng. 2018. When will you arrive? Estimating travel time based on deep neural networks. In *Proceedings of the AAAI Conference on Artificial Intelligence*, Vol. 32.
- [27] Jingyuan Wang, Jiawei Jiang, Wenjun Jiang, Chao Li, and Wayne Xin Zhao. 2021. LibCity: An Open Library for Traffic Prediction. In *Proceedings of the 29th International Conference on Advances in Geographic Information Systems (Beijing, China) (SIGSPATIAL '21)*. Association for Computing Machinery, New York, NY, USA, 145–148. <https://doi.org/10.1145/3474717.3483923>
- [28] Senzhang Wang, Meiyue Zhang, Hao Miao, Zhaohui Peng, and Philip S Yu. 2022. Multivariate correlation-aware spatio-temporal graph convolutional networks for multi-scale traffic prediction. *ACM Transactions on Intelligent Systems and Technology (TIST)* 13, 3 (2022), 1–22.
- [29] Ning Wu, Xin Wayne Zhao, Jingyuan Wang, and Dayan Pan. 2020. Learning effective road network representation with hierarchical graph neural networks. In *Proceedings of the 26th ACM SIGKDD international conference on knowledge discovery & data mining*. 6–14.
- [30] Zonghan Wu, Shirui Pan, Guodong Long, Jing Jiang, Xiaojun Chang, and Chengqi Zhang. 2020. Connecting the dots: Multivariate time series forecasting with graph neural networks. In *Proceedings of the 26th ACM SIGKDD international conference on knowledge discovery & data mining*. 753–763.
- [31] Zonghan Wu, Shirui Pan, Guodong Long, Jing Jiang, and Chengqi Zhang. 2019. Graph wavenet for deep spatial-temporal graph modeling. (2019), 1907–1913.
- [32] Haoyang Yan, Xiaolei Ma, and Ziyuan Pu. 2021. Learning dynamic and hierarchical traffic spatiotemporal features with transformer. *IEEE Transactions on Intelligent Transportation Systems* (2021).
- [33] Huaxiu Yao, Yiding Liu, Ying Wei, Xianfeng Tang, and Zhenhui Li. 2019. Learning from Multiple Cities: A Meta-Learning Approach for Spatial-Temporal Prediction. In *the Web Conference 2019 (WWW'19)*.
- [34] Bing Yu, Haoteng Yin, and Zhanxing Zhu. 2018. Spatio-temporal Graph Convolutional Networks: A Deep Learning Framework for Traffic Forecasting. In *Proceedings of the 27th International Joint Conference on Artificial Intelligence (IJCAI)*.
- [35] Fisher Yu and Vladlen Koltun. 2015. Multi-scale context aggregation by dilated convolutions. *arXiv preprint arXiv:1511.07122* (2015).
- [36] Bohang Zhang, Shengjie Luo, Liwei Wang, and Di He. 2023. Rethinking the Expressive Power of GNNs via Graph Biconnectivity. (2023). <https://openreview.net/forum?id=r9hNv76KoT3>
- [37] Junbo Zhang, Yu Zheng, and Dekang Qi. 2017. Deep spatio-temporal residual networks for citywide crowd flows prediction. In *Proceedings of the AAAI conference on artificial intelligence*, Vol. 31.
- [38] Junbo Zhang, Yu Zheng, Junkai Sun, and Dekang Qi. 2019. Flow prediction in spatio-temporal networks based on multitask deep learning. *IEEE Transactions on Knowledge and Data Engineering* 32, 3 (2019), 468–478.
- [39] Zijian Zhang, Xiangyu Zhao, Hao Miao, Chunxu Zhang, Hongwei Zhao, and Junbo Zhang. 2023. AutoSTL: Automated Spatio-Temporal Multi-Task Learning. *Proceedings of the AAAI Conference on Artificial Intelligence* 37, 4 (Jun. 2023), 4902–4910. <https://doi.org/10.1609/aaai.v37i4.25616>
- [40] Ling Zhao, Yujiao Song, Chao Zhang, Yu Liu, Pu Wang, Tao Lin, Min Deng, and Haifeng Li. 2019. T-gcn: A temporal graph convolutional network for traffic prediction. *IEEE transactions on intelligent transportation systems* 21, 9 (2019), 3848–3858.
- [41] Xiangyu Zhao, Wenqi Fan, Hui Liu, and Jiliang Tang. 2022. Multi-Type Urban Crime Prediction. In *Proceedings of the AAAI Conference on Artificial Intelligence*, Vol. 36. 4388–4396.
- [42] Xiangyu Zhao and Jiliang Tang. 2017. Modeling Temporal-Spatial Correlations for Crime Prediction. In *Proceedings of the 2017 ACM on Conference on Information and Knowledge Management*. ACM, 497–506.
- [43] Xiangyu Zhao and Jiliang Tang. 2018. Crime in Urban Areas: A Data Mining Perspective. *ACM SIGKDD Explorations Newsletter* 20, 1 (2018), 1–12.
- [44] Xiangyu Zhao, Tong Xu, Yanjie Fu, Enhong Chen, and Hao Guo. 2017. Incorporating Spatio-Temporal Smoothness for Air Quality Inference. In *2017 IEEE International Conference on Data Mining (ICDM)*. IEEE, 1177–1182.
- [45] Chuanpan Zheng, Xiaoliang Fan, Cheng Wang, and Jianzhong Qi. 2020. Gman: A graph multi-attention network for traffic prediction. In *Proceedings of the AAAI conference on artificial intelligence*, Vol. 34. 1234–1241.
- [46] Zibin Zheng, Yatao Yang, Jiahao Liu, Hong-Ning Dai, and Yan Zhang. 2019. Deep and embedded learning approach for traffic flow prediction in urban informatics. *IEEE Transactions on Intelligent Transportation Systems* 20, 10 (2019), 3927–3939.